buildings

MDPI

Article

Structural Performance Assessment of Innovative Hollow Cellular Panels for Modular Flooring System

Keerthana John [1,*], Sherin Rahman [1], Bidur Kafle [1], Matthias Weiss [2], Klaus Hansen [3], Mohamed Elchalakani [4], Nilupa Udawatta [5], M. Reza Hosseini [5] and Riyadh Al-Ameri [1]

1 School of Engineering, Deakin University, Geelong, VIC 3217, Australia; skrahman@deakin.edu.au (S.R.); bidur.kafle@deakin.edu.au (B.K.); r.alameri@deakin.edu.au (R.A.-A.)
2 Institute for Frontier Materials, Deakin University, Geelong, VIC 3217, Australia; matthias.weiss@deakin.edu.au
3 L2U Pty. Ltd., Perth, WA 6017, Australia; klaus@nksom.com
4 Civil, Environmental and Mining Engineering, The University of Western Australia, Perth, WA 6009, Australia; mohamed.elchalakani@uwa.edu.au
5 School of Architecture & Built Environment, Deakin University, Geelong, VIC 3217, Australia; nilupa.udawatta@deakin.edu.au (N.U.); reza.hosseini@deakin.edu.au (M.R.H.)
* Correspondence: johnke@deakin.edu.au

Abstract: Lightweight modular construction has become an increasing need to meet the housing requirements around the world today. The benefits of modular construction ranging from rapid production, consistency in quality, sustainability, and ease of use have widened the scope for the construction of residential, commercial, and even emergency preparedness facilities. This study introduces novel floor panels that can be flat-packed and built into modular housing components on-site with minimal labour and assistance. The flooring system uses hollow cellular panels made of various configurations of trapezoidal steel sheets. The structural performance of three different configurations of these hollow flooring systems as a modular component is presented in this study by analysing the failure modes, load-displacement parameters, and strain behaviour. The study confirms significant advantages of the proposed hollow floor systems, with multi-cells reporting higher load-carrying capacity. The hollow flooring system performed well in terms of structural performance and ease in fabrication as opposed to the conventional formworks and commercial temporary flooring systems. The proposed flooring system promises efficient application as working platforms or formworks in temporary infrastructural facilities and emergency construction activities.

Keywords: cellular flooring; modular construction; profiled sheets; structural performance

Citation: John, K.; Rahman, S.; Kafle, B.; Weiss, M.; Hansen, K.; Elchalakani, M.; Udawatta, N.; Hosseini, M.R.; Al-Ameri, R. Structural Performance Assessment of Innovative Hollow Cellular Panels for Modular Flooring System. *Buildings* **2022**, *12*, 57. https://doi.org/10.3390/buildings12010057

Academic Editor: Jian-Guo Dai

Received: 14 December 2021
Accepted: 5 January 2022
Published: 6 January 2022

1. Introduction

The construction of an emergency housing system is still one of the priorities in the 21st century for many humanitarian and government agencies due to various natural disasters and civilian crises. It is estimated that approximately 260 million people migrate to different parts of the globe, creating increased demand in the housing sector [1]. With an anticipated increase in these numbers, it is high time for the construction sector to fast track research on affordable, fast-paced, modular and adaptable housing systems to meet the needs of the future generation [1,2]. The construction sector has strived to address such increased demand, and hence the focus is to develop thoughtful innovations in construction, method, technology and equipment [2,3]. The adoption of offsite construction is one such innovation in the construction industry that enables the workers and machinery to work in a controlled environment. Offsite construction has also increased productivity, quality and safety due to reduced external influences on the construction stage [4].

Offsite construction is the future of the building industry, where construction processes resemble manufacturing procedures and construction sites are used only for assembling

modular building components [5]. In this construction method, the whole structure can be assembled with prefabricated components that can be transported and installed on-site [6,7]. The prefabricated modules can include beams, columns, slabs, stairs, and panel elements of various construction materials, including concrete, steel, timber, or composite materials [6,8]. This method has several benefits such as improved quality, enhanced structural reliability and productivity. It also reduces the construction time, labour and wastage because of the controlled environment under which they are manufactured [9,10]. The modular construction process incorporates design optimisation, and there is an opportunity to reuse the building components effectively [11]. Thus, the modular construction method aligns with circular economy principles and ensures that all building components fulfil structural performance requirements, building codes, and standards [12,13].

Modular construction is also highly conducive to supporting sustainability initiatives. Considering these aspects, lightweight steel modular units are becoming popular for constructing emergency facilities due to their acceptable structural performance, fire resistance and lightweight characteristics [14]. These modular steel components have shown enhanced strength and rigidity, as evidenced by various studies [9,15]. However, there is a need of designing effective connections for assembling the modular components. Steel modular structures with easy connectors are a good alternative for immediate response for the industry [2,8]. Despite several advantages of modular construction over the conventional construction process, the structures industry still rely heavily on the traditional on-site construction methods [4,9]. There is a lack of lightweight, integrated, and reconfigurable building components, especially floor systems [16]. A review of the existing literature suggests enormous potential for investigating the structural efficacy of hollow flooring systems made of lightweight corrugated steel sheets [17]. Some studies indicate that the use of profiled steel sheets is increasing to provide quality and affordable housing in the form of self-supporting roofs and other applications owing to their structural capabilities without any support [11,18]. Experimental investigation of profiled steel sheets for their constructability in various applications such as composite flooring systems have shown encouraging results [19,20].

This experimental research develops a novel modular flooring system with L2U Group Pty Ltd. (L2U) from Perth, Australia, FormFlow [21], Geelong, Australia and Deakin University, from Geelong, Australia. This study specifically focused on developing floor hollow floor decks from simple trapezoidal corrugated sheets for temporary structural applications in the emergency housing sector. The prototypes of the flooring panel were made using flat-packed corrugated sheets supplied by L2U Group Pvt. Ltd., Perth, Australia which were then assembled in the Deakin University laboratory facility in Geelong. This paper presents the test results of the structural performance of three different cell configurations of the novel floor panels. Detailed analysis of the load-displacement behaviour, failure modes and strain data of various panel configurations and their assessment for suitability in temporary floor construction is presented.

2. Materials and Methods

The test program fabricates the innovative cellular panels from corrugated profile sheets. It tests their performance as a temporary floor panel for emergency housing and as a working platform for other construction applications. The fabrication of the cellular panel from the flat-packed profile sheets was conducted following the U.S. Patent 8,539,730 B2 [22]. In total, four different hollow cell configurations were identified to investigate the performance in various arrangements, two of them are single cell, and two were multi-cell arrangements.

Hence, the current proposal introduces and tests a method for simple flooring made using an overlapping pattern of locally available corrugated sheets [21]. It enables the construction of a flooring system even in an irregular terrain ruling out the need for initial site preparation [21]. Moreover, this type of flooring does not require skilled labour and

can be used with ease, especially for emergency structures such as in refugee shelters and temporary housing platforms.

2.1. Fabrication of the Innovative Hollow Cellular Panels

The hollow panels made of simple trapezoidal profiled corrugated sheets (Figure 1a) were fabricated by L2U Pty. Ltd., a start-up company in Western Australia with the assistance of FormFlow for prototyping, design, and logistics. FormFlow is a leading Australian developer of advanced steel building solutions and recently patented a world-first technology to produce sharp 90 degree bends in corrugated sheets; the product has been commercialised in Australia as Lysaght CUSTOMFLOW [23]. A simple trapezoidal-corrugated steel strip commonly employed in roof or wall cladding throughout Australia has been adopted by L2U for the new system. The flat-packed sheets provided for this study were 1200 mm (L) × 600 mm (W) sizes with 0.42 mm sheet thickness. All the materials used in the study were provided by our industry partner—L2U group Pvt. Ltd., Perth, Australia. These are commercially available as Lysaght Trimdek, which is a commonly used trapezoidal corrugated steel sheet. The corrugated steel used is coated with ZINCALUME (aluminium/zinc/magnesium alloy) which complies with AS1397:2011. The sheet offers yield strength of 550 MPa with a coating mass of 125 g/m^2. These details are provided by the manufacturer for the purpose of our study [24].

The sheets are then bent along the axis of the slots at 90°, as shown in Figure 1a. Custom slots are provided along the longitudinal direction of the sheet (Figure 1b,c) at the required distance using the Computerised Numerical Control or CNC cutting technique for ease of bending at ends. The flat-packed corrugated sheets are bent halfway into a 'C' shaped panel section, which can be laid over the adjacent panels until the desired span is achieved and closed at the end section by fasteners or bolts. Plates can also be included at the end of the middle section of the panels to provide improved structural integrity (Figure 1d). Multiple sheets for longer spans can also be fabricated and connected this way. When folded over the adjacent cell, an overlap is formed at the folds, and this configuration results in the cells being significantly robust, as shown in Figure 1e. The end plates connect the top and bottom skins of the steel sheets to form a complete cell.

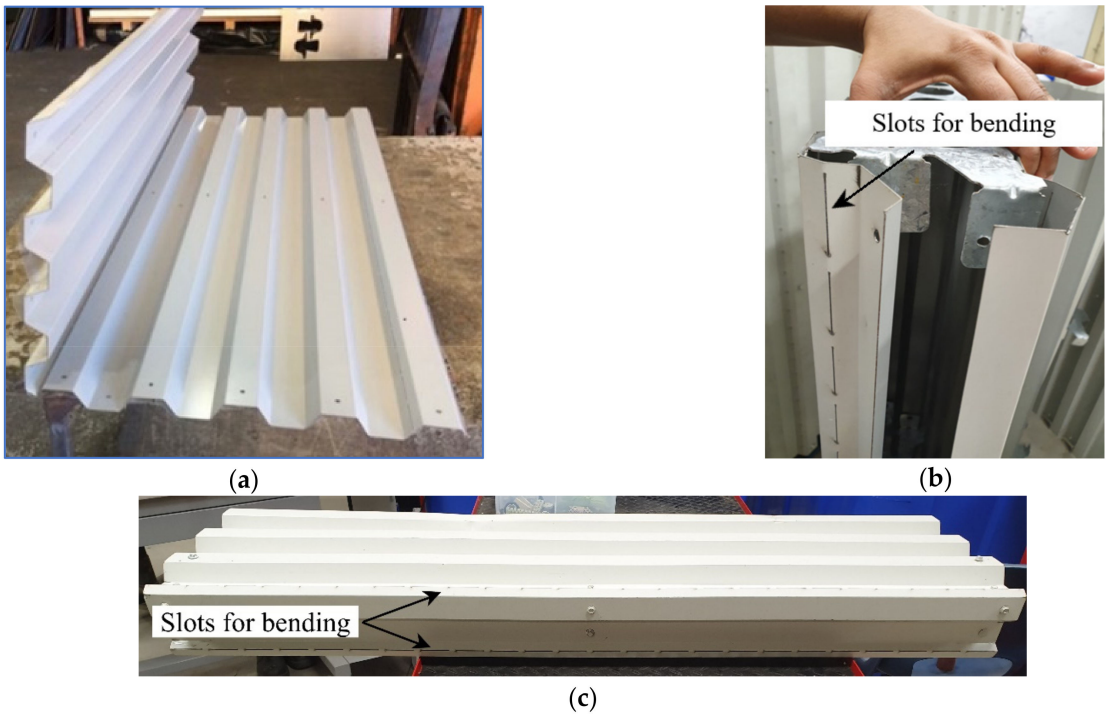

(**a**) (**b**)

(**c**)

Figure 1. *Cont.*

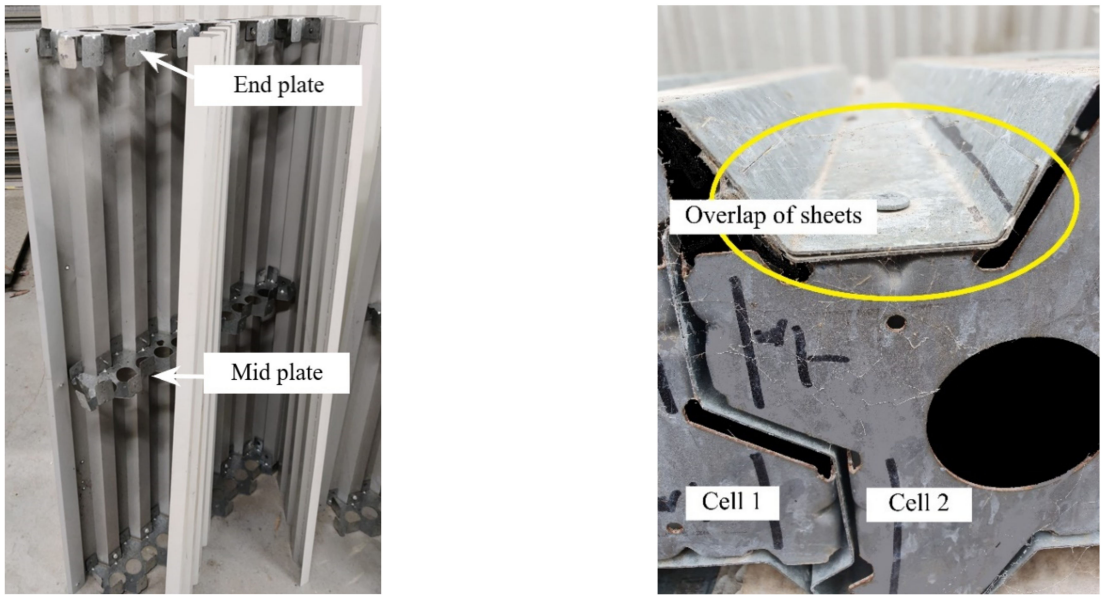

(**d**) (**e**)

Figure 1. Prototype of hollow cellular panel. (**a**) Bent 'L' shaped corrugated sheet. (**b**) Slots for bending at open end. (**c**) Slots for bending at corrugation edges. (**d**) Open panel with mid plates (**e**) Overlap of sheets of a multi-cell panel.

2.2. Panel Details

This study investigates three different panel configurations: a single cell, a double cell, and a triple cell (shown in Figure 2). The details of the test specimens' dimensions, panel types, and configurations are provided in Table 1.

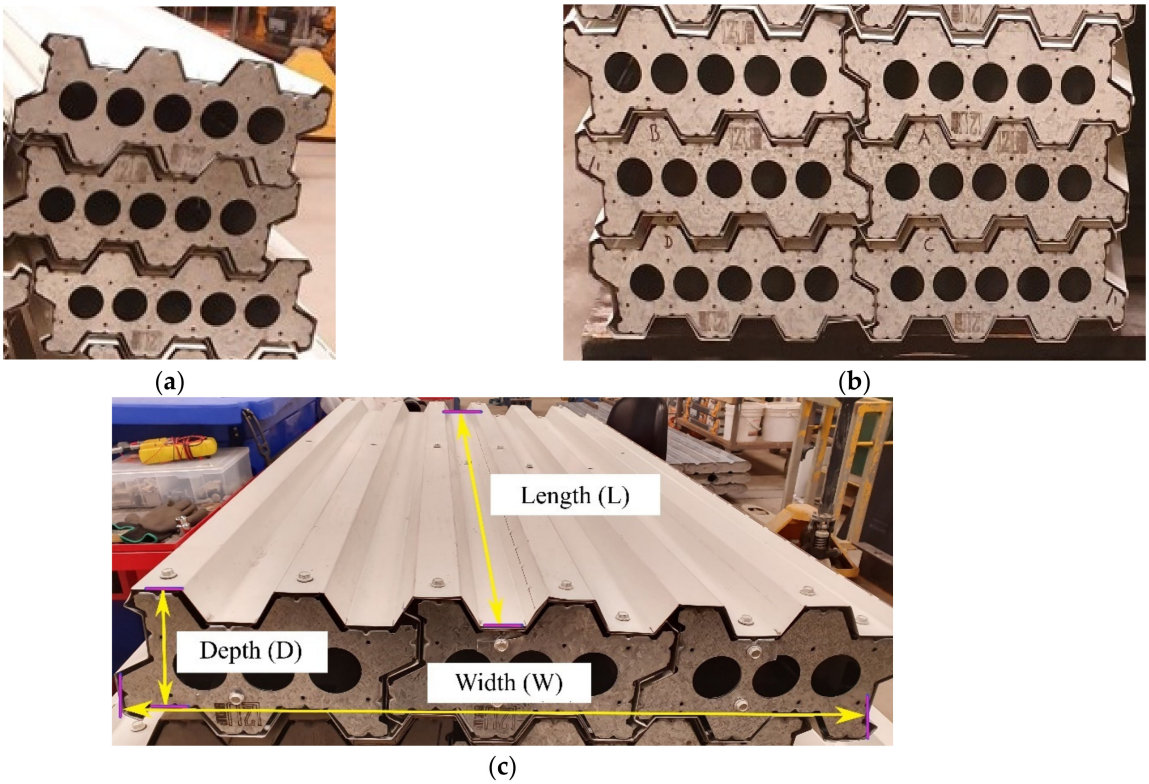

(**a**) (**b**)

(**c**)

Figure 2. (**a**) Single-cell panels. (**b**) Double cell panels. (**c**) Triple Cell Panels with annotations of dimensions used.

Table 1. Details of Test Specimens.

Panel Type	Panel ID	Panel Dimensions (L × W × D) mm	Width of Individual Cell (W) mm	Number of Panels Tested
Single cell (with mid-plate)	SC-P	1200 × 300 × 100	300	2
Single cell (without mid-plate)	SC	1200 × 300 × 100	300	1
Double cells (without mid-plate)	DC	1200 × 600 × 100	300	2
Triple cells (without mid-plate)	TC	1200 × 600 × 100	200	2
Total number of panels				7

Out of the above test specimens, a couple of single cells were provided with a mid-plate to assess its role in the structural behaviour of the panel for initial investigation. The mid-plate position is shown in Figure 1d. This plate is made of steel, cut to the panel's shape, and is provided at the centre of the panels at 600 mm as a support element. Multi-cell panels were tested without mid-plates to achieve a complete hollow cellular system. It was assumed that the overlap of sheets in multi-cell panels would enhance the structural efficiency eliminating the need for mid-plates. Thus, the multi-cell panels were kept at a constant total width of 600 mm with an individual cell width of 300 mm for double cell panels and 200 mm for the triple cell panels to assess the structural performance of the overlapping sheet system. Another aim of testing multi-cell panels with different cell widths was to observe the role of various cell configurations in their overall structural behaviour as a flooring system.

2.3. Test Set-Up

A four-point bending arrangement was followed to test the hollow cellular panels as depicted in Figure 3a,b. The panels were simply supported at an effective span of 1000 mm. The load was applied at the mid-span through a hydraulic piston onto roller supports at 334 mm spacing from each other. The test was displacement controlled at the rate of 2.5 mm/min. A laser transducer was placed underneath the panel at the centre of the panel to measure the mid-point displacement. Electrical resistance strain gauges were positioned at the top and bottom of the panel. Three strain gauges were positioned at the bottom of the panel: SG1 and SG3 below the load points and SG2 at the centre of the panel. At the same time, SG4 was placed at the centre of the top skin of the panel (Figure 3d). A data acquisition system connected to the load frame was programmed to capture the applied load, displacement, and strain data. The panels were supported by timber blocks positioned in the panels and above the supports, as shown in Figure 3c. It was done to prevent the primary crushing of corrugations when the load is applied and to ensure an appropriate failure mode.

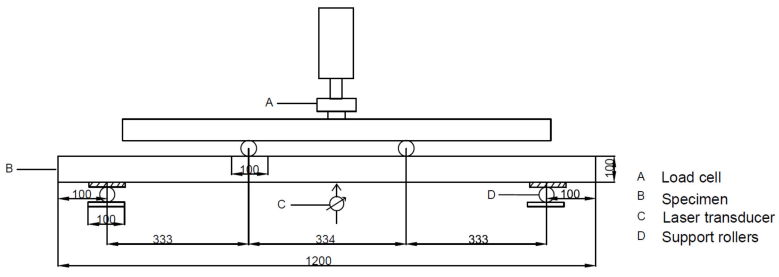

(**a**)

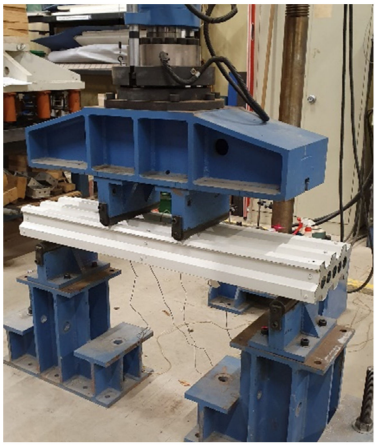

(**b**)

Figure 3. *Cont.*

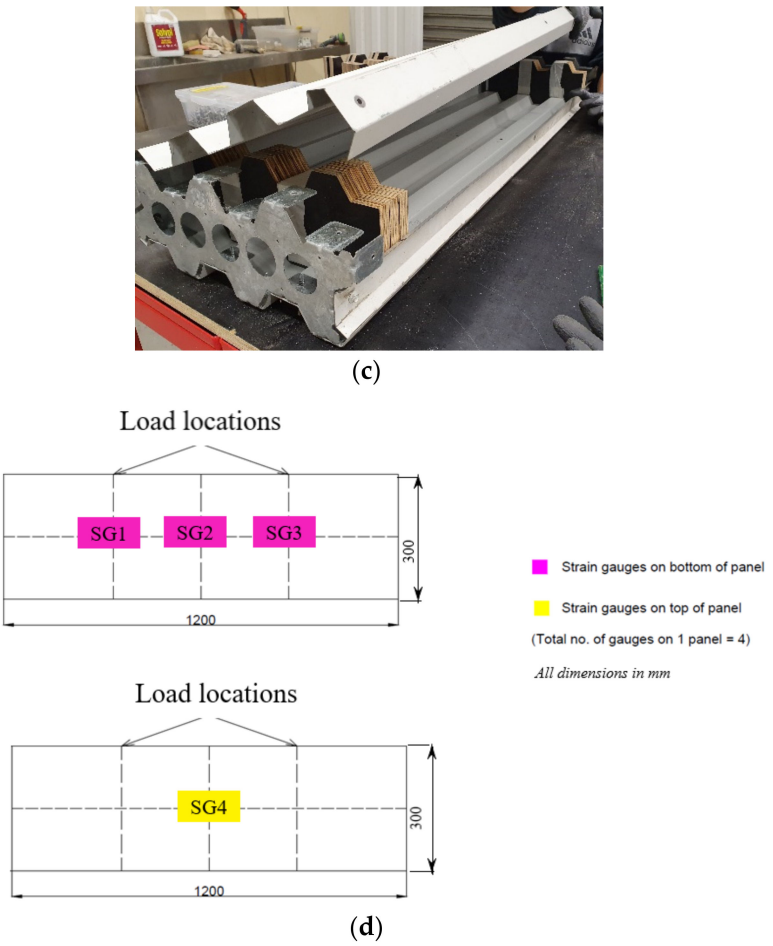

Figure 3. (**a**) Test set-up for panels. (**b**) Test arrangement of the single-cell panel. (**c**) Open panel with timber blocks inserted over end support regions. (**d**) Position of strain gauges.

3. Results and Discussion

3.1. Load-Displacement Behaviour

3.1.1. Single-Cell Panels

Both single-cell panels with mid-plate (SC-P) attained an average ultimate load of 6.34 kN, which is 76% higher than the panel without mid-plate (SC) which had an ultimate load of 3.60 kN. It suggests that the mid-plate contributes to a significant load-carrying capacity of the panels. The mid-plate also mobilises the contribution of the lower sheet in load-carrying capacity at the early stages of loading. In the panels without a mid-plate, the lower sheet will only take part in load resistance at the later stages of loading due to the lack of connectivity with the top plate. It is seen from Figure 4 that all single-cell panels exhibit excellent ductile behaviour.

In SC-P panels, the load is maintained due to mid-plate and gradually decreases when the skins buckled over the mid-plate. However, the load does not undergo any significant reduction in the SC panel and continues steadily to carry the load until the test is stopped at 90 mm displacement. The panel has already suffered local buckling at this stage, and high displacements were attained. Hence irrespective of the load-carrying capacity, the test was stopped at this stage. The top skin of the panel acted independently due to the absence of a mid-plate to transfer the load to the bottom skin. Once it touched the bottom skin, the ultimate load-carrying capacity was maintained due to double skin action, seen from the load-displacement graph in Figure 4 and Table 2.

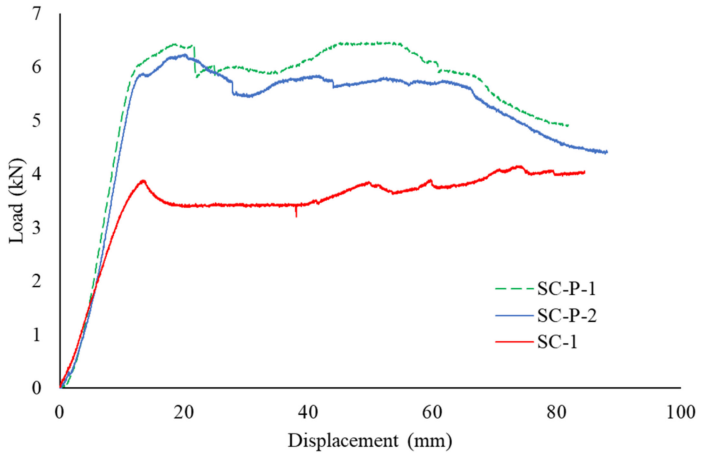

Figure 4. Load vs. displacement of single-cell panels.

Table 2. Results of single cell panel tests.

Panel	Ultimate Load (kN)	Displacement—Top Skin (mm)	Displacement—Bottom Skin (mm)
SC-P-1	6.23	20.10	19.98
SC-P-2	6.46	21.13	21.15
Average	6.34	20.61	20.56
SC	3.60	15.30	0.91

To further investigate the role of the double skin action in the SC panel, the load-displacement relationship of the top and bottom skins is plotted as shown in Figure 5. Double skin action of the panels here is defined as the load carrying capacities created by the top and bottom skins when acting together.

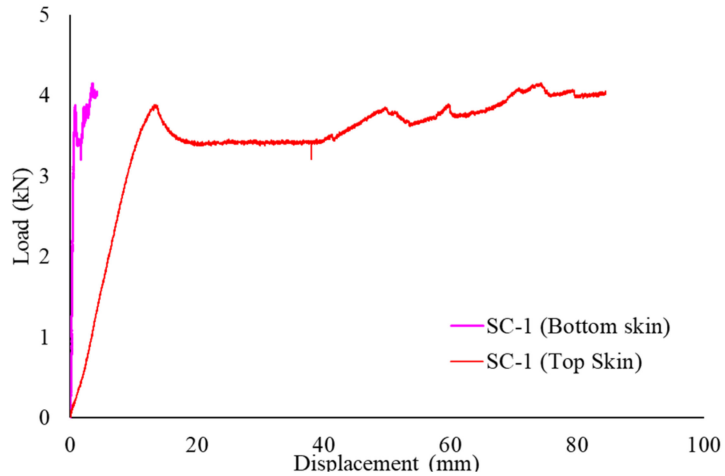

Figure 5. Load vs. displacement of top and bottom skins in SC panel.

Displacement on the top skin is significantly high, whereas the bottom skin started to deflect later without any noticeable amount compared with the top skin. During the test, the displacement in the bottom skin was initiated only after the top skin touched the bottom skin. This observation is evidenced by the bottom and top skin displacement at ultimate loads as 0.91 mm and 15.30 mm, respectively (Table 2). It implies that the mid-plate contributed to distributing loads and displacements between the top and bottom skins.

3.1.2. Multi-Cell Panels

The load-displacement behaviours of both double and triple cells are presented in Figure 6.

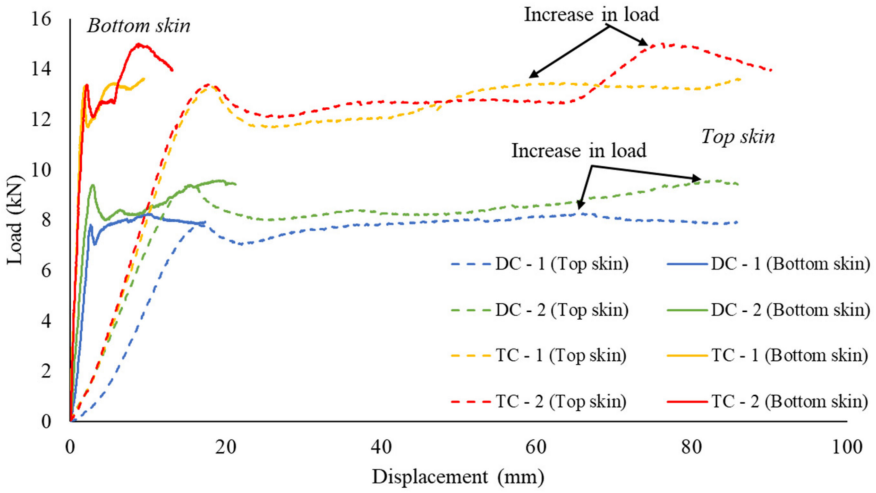

Figure 6. Load vs. displacement of multi-cell panels.

It is evident from Figure 6 that the triple cell panels attained a significantly higher average ultimate load of 13.34 kN compared to double cell panels with an average ultimate load of 8.6 kN. There is around a 55% increase in the ultimate load-carrying capacity from the double to triple cells owing to the additional partitioning steel walls in the 600 mm cross-sections of the triple cell panels. Hence it is evident that any addition of cells multiplies the load capacity due to additional overlap of sheets. Like single-cell panels, excellent ductile behaviour was seen for all panels, as shown in Figure 6. Ultimate load is achieved at a lower displacement and a steady load without considerable load reduction. When the top skin touches the bottom skin, the maximum load is again achieved as indicated in the graphs as increased load, and the test is terminated at 90 mm displacement. The displacement measured on the bottom skin indicates that this skin is only activated at the later stages and undergoes minor displacement, similar to the single-cell panel (SC). The test results are compiled in Table 3 below.

Table 3. Results of multi-cell panel tests.

Panel	Panel Dimensions (mm)	Width of Individual Cell (mm)	Number of Cells	Ultimate Load (kN)	Displacement—Top Skin (mm)	Displacement—Bottom Skin (mm)
DC—1	1200 × 600 × 100	300	2	7.81	16.46	2.61
DC—2	1200 × 600 × 100	300	2	9.38	15.47	2.86
		Average		8.59	15.96	2.73
TC—1	1200 × 600 × 100	200	3	13.30	18.03	1.78
TC—2	1200 × 600 × 100	200	3	13.38	17.77	2.12
		Average		13.34	17.90	1.95

3.1.3. Summary of Load-Displacement Behaviour

Adopting single, double, and triple cell configurations helped in understanding the load distribution in the different panels. The strength multiplication in the double cells of 600 mm width from the single cells of 300 mm width confirm that the one-way slab action is maintained for all the slab configurations used in this study. Furthermore, when the mid-plates are provided for the single-celled panel configuration (SC-P), the load-carrying capacity increases by 76% compared with the single-celled panels without mid-plate (SC).

From the load-displacement curves, it is evident that any addition of cell numbers creates a more stiffened panels, thereby multiplying the load-carrying capacity of the proposed

innovative flooring system. The strength improvement is therefore due to the overlapping action in the multi-celled panels. In the current test program, the triple celled panels achieved 55% higher ultimate loads than the double celled panels even though both had the same overall dimensions of 1200 mm (L) × 600 mm (W) and 100 mm depth (D).

Table 4 is shown for further comparison of the performance of the 300 mm wide single cells and 600 mm wide double cells.

Table 4. Comparison of average load vs displacement values for single cell and double cell panels.

Panel	Panel Dimensions (mm)	Width of Individual Cell (mm)	No. of Cells	Ultimate Load (kN)	Displacement—Top Skin (mm)	Displacement—Bottom Skin (mm)
Single Cell (Without mid-plate)	1200 × 300 × 100	300	1	3.60	15.30	0.91
Single cell (With mid-plate)	1200 × 300 × 100	300	1	6.34	20.61	20.56
Double Cell	1200 × 600 × 100	300	2	8.59	15.96	2.73

From Table 4 it is clear that on multiplying the cell numbers, there is significant increase in the load capacity, however maintaining the one-way load distribution irrespective of the doubling of cells. A 35.50% increase is seen between single cells with mid-plates and double cells without mid-plate, however, the panel with mid-plates reported higher displacements. The mid-plates are therefore beneficial for higher load carrying applications and ensures complete utilization of the top and bottom skins of the panels for load transfer.

To further investigate the effect of overlapping on multi cell panels with same overall dimensions, ultimate load, and displacement on two types of multi cells (double and triple) panels have been compared and presented in Table 5. The triple cell panel achieved 55% more ultimate load compared with double cell panel with similar overall dimensions, confirming the benefits of additional partitioning walls. On the other hand, the displacements at top and bottom skins are comparable on both double and triple cells, indicating that triple cell can resist more loads without significant increase in displacement.

Table 5. Comparison of average load vs. displacement values for double cell and triple cell panels.

Panel	Panel Dimensions (mm)	Width of Individual Cell (mm)	No. of Cells	Ultimate Load (kN)	Displacement—Top Skin (mm)	Displacement—Bottom Skin (mm)
Double Cell	1200 × 600 × 100	300	2	8.59	15.96	2.73
Triple cell	1200 × 600 × 100	300	3	13.34	17.90	1.95

The results from these tests confirm that the current design of panels ensures structural adequacy in carrying construction loads. Thus, it implies that the proposed panel's configurations are adequate for the application in temporary structures for formwork, emergency shelters, etc.

3.2. Failure Mode

3.2.1. Single-Cell Panels

Panels with Mid-Plate

The mid-plate in single-cell panels, SC-P, provided an excellent resistance to load. Flexural failure of the panel (Figure 7a), local buckling around the mid-plate (Figure 7b) and below the loading point (Figure 7c) were observed. The slots provided for bending of the sheets also suffered tearing at these critical points. The failure of slots can be attributed to compression of the top skin of the panel over the mid-plate. This behaviour was noticed towards the end of the test when large displacement values beyond 50 mm were already attained. The top skin of the panels also began to separate from the endplates due to these high displacements, as shown in Figure 7d. However, it was observed that the mid-plate

was acting as a medium to transfer the load from top skin to bottom skin of the panel and hence the full capacity of the panel was exploited.

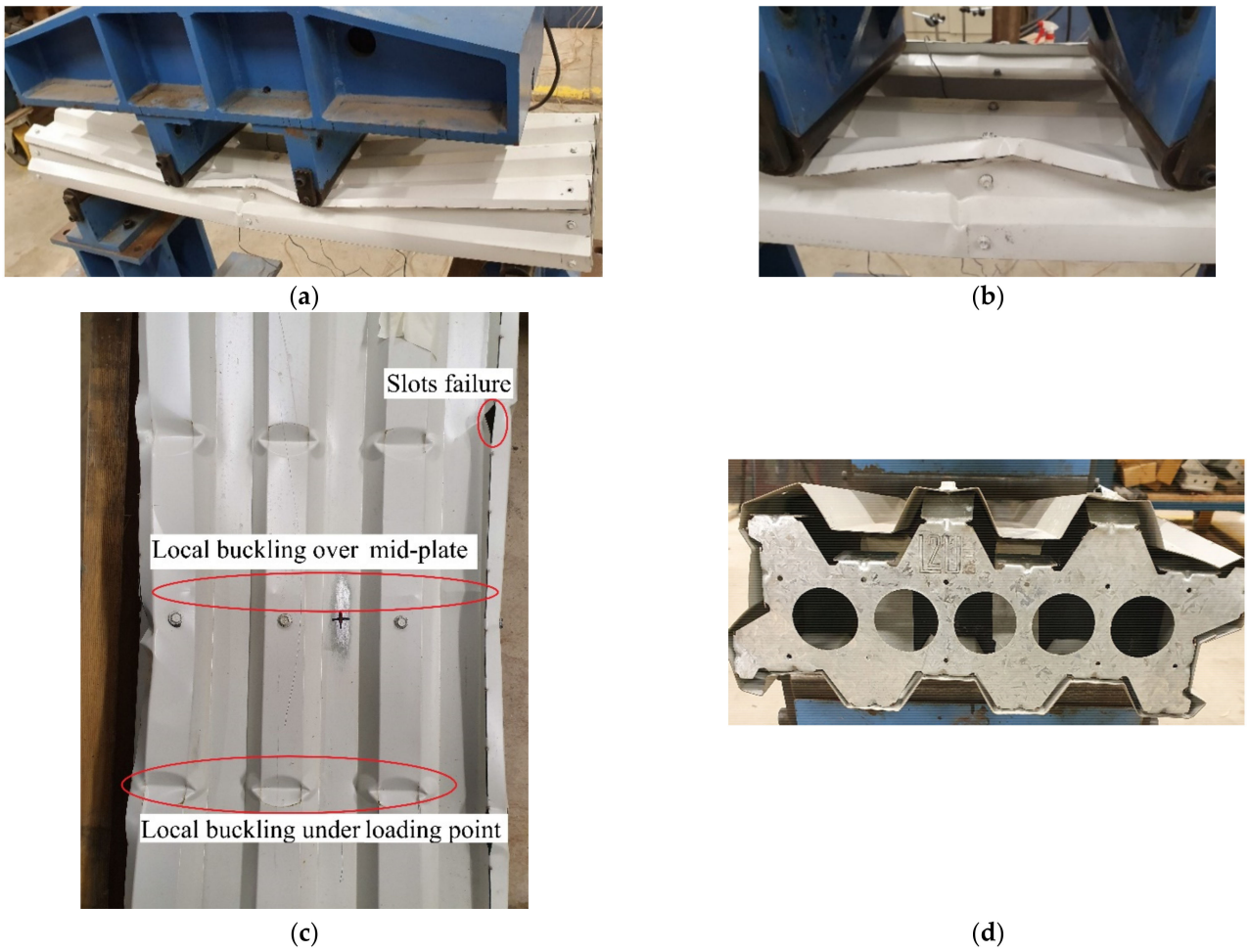

Figure 7. (**a**) Failed SC-P panel. (**b**) Buckling over mid-plate in SC-P. (**c**) Failure points on SC-P panel (**d**) Separation of panel skin from endplates.

Panels without Mid-Plate

The panel without the mid-plate also failed by flexure (Figure 8a). However, local buckling was noticed only below the load points. It is seen from Figure 8b that only the top skin of the panel suffered failure while the bottom skin remained significantly undamaged. Similar to panels with mid-plates, separation of the skins from the endplate was noticed at higher displacement beyond 50 mm.

(**a**)

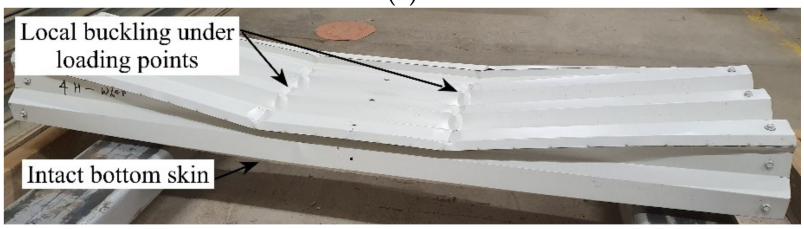

(**b**)

Figure 8. (**a**) Failure of SC panel. (**b**) Failed SC panel with the intact bottom skin.

3.2.2. Multi-Cell Panels

The failure modes of both double and triple cell panels were very similar, and both underwent flexural failure (Figure 9a). All multi-cell panels experienced the same failure behaviour. Local buckling was noticed only under the load points, as shown in Figure 9b, without any failure of the slots. The top and bottom skin acted independently, and hence the bottom skin was not affected by any local failure and remained undamaged (Figure 9c). However, the bottom skins flattened themselves (Figure 9d) at the slots, which deformed the panel along the centre. It commenced when the top skin began touching the bottom skin due to displacement. The overlap in one of the double cell panels suffered separation at the centre of the panel due to high displacement (Figure 9e). However, this was not observed in the case of the triple cells. Consistent with single-cell panels, the top skin began detaching from the endplate when higher displacements of over 50 mm were initiated.

(**a**)

(**b**)

Figure 9. *Cont.*

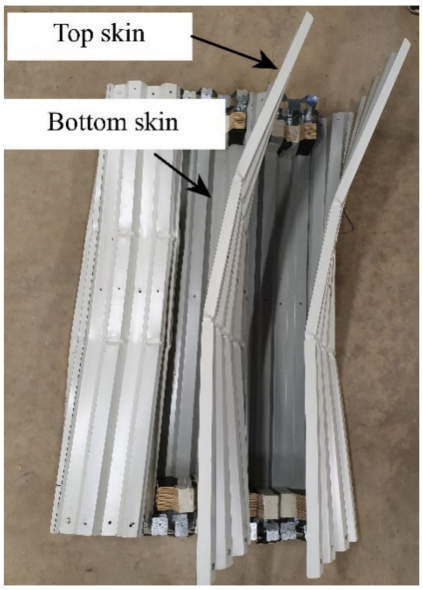

(**c**)

(**d**)

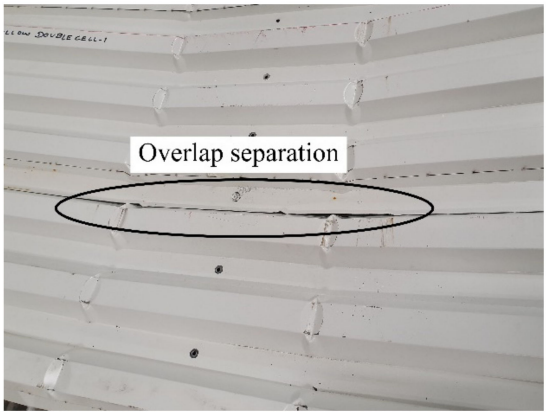

(**e**)

Figure 9. (**a**) Failed double cell panel. (**b**) Local buckling in triple cell panel. (**c**) Open triple cell sample with the intact bottom skin. (**d**) Flattening of bottom skin at slots. (**e**) Separation at the overlap of double cell-1.

3.2.3. Summary of Failure Mode Results

The failure modes for the four different configurations of multi-cell panels and single cells were analysed. It is found that local buckling was a noticeable failure mode in all the specimens irrespective of the number of cells. The other observed failure type was the slot failure with single-cell containing mid-plates, which might be because of deformation around the mid-plates. However, there was no local buckling in the bottom skin of the single cells without mid-plates which indicates the lack of effective load transfer between the two skins of the panel. In the case of multi-cells, there was no significant

separation between the individual cells despite recording local buckling, which can be attributed to the efficient overlay of the sheet panels. It is to be noted that both double and triple cell panels failure modes were similar in all specimens tested. Analysis of failure modes recommends the need for mid-plates or any other infill medium to enhance the efficiency of the proposed panel sections for flooring. It is recommended to fill the voids with some cementitious material so that this system can be further used in structural applications as a flooring system. The infill component will assist efficient use of both top and bottom skins in resisting load and avoiding failure of only top skin.

3.3. Load-Strain Distribution

3.3.1. Single-Cell Panels

The load-strain curves for SC-P and SC panels are shown in Figure 10. The strains were measured at the centre of the panel on the top and bottom skins and underneath a loading point on the bottom skin. In Figure 10a the top of the SC-P panel remains in compression while the bottom of the panel continues in tension due to the action of the mid-plate. The point under the load also remains in tension in the bottom skin. Equal action of top and bottom skins can be observed due to similar strain distribution in both skins with increasing load value.

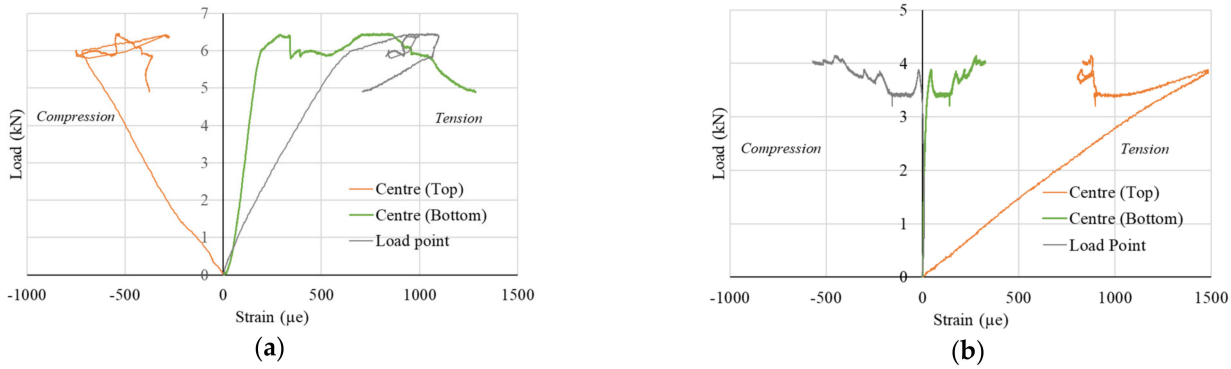

Figure 10. (**a**) Load vs. strain curves of SC-P panel. (**b**) Load vs. strain curves of SC panel.

In contrast, the top skin continues in tension until it touches the bottom skin of the SC panel, after which distortion is seen in the strain (Figure 10b). After this point, the bottom skin experiences minor tensile strain. This behaviour was observed once the top skin touched the bottom skin and can be seen from the green colour plot in Figure 10b. The lack of combined action of the double skin can also be noticed from the strain under the load point, which only began when the ultimate load was achieved. The results indicate that the middle plate in SC-P utilised the entire panel capacity to act as a whole. In contrast, the load-carrying capacity of the SC panels was lower than that of the SC-P panel, where each skin acted independently.

3.3.2. Multi-Cell Panels

Top skin shows a steady rise in tensile strain until it touches the bottom skin, after which a distortion by reduction of strain is noticed in both double and triple cell panels (Figure 11). The bottom skin begins a significant increase in strain only at this point, and the points under the load also begin transferring load at this point. This action is like the SC panels, which is also without a mid-plate. A compression behaviour is recorded under the load point in the triple celled panels because of the extended sheet overlap on the panels.

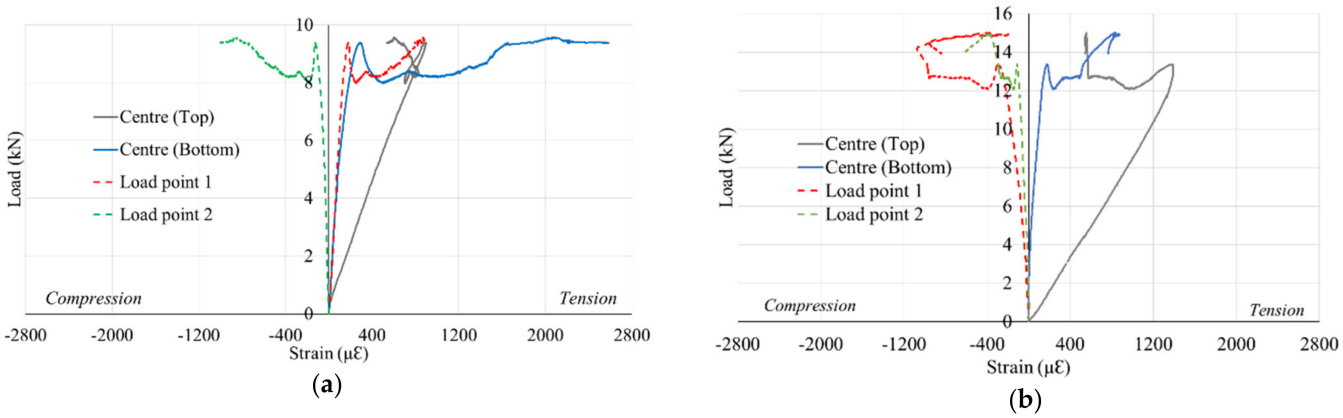

Figure 11. (**a**) Load vs. strain curves of double cell panel. (**b**) Load vs. strain of triple cell panel.

3.3.3. Summary of Load–Strain Behaviour

The load–strain curves were analysed to record the variations in the panel behaviour and identify the critical points of failure. From strain measurements on either side of the panels to monitor the individual behaviour of the top and bottom skins, it is evident that in the panels with mid-plate, the top and bottom skins reported similar behaviour with identical performance in the tension and compression zones. However, in the case of the panels without the mid-plate, the bottom skin started recording significant strains only after the top skin reached its maximum tension capacity. This behaviour indicates the double-skinned action is enhanced and efficient only with mid-plates or any other medium to distribute the loads between the top and bottom skins of the hollow panels.

4. Conclusions

This experimental study confirms the feasibility of adopting the newly proposed innovative flooring systems for temporary structures such as working platforms or formworks. The multi-celled panel systems promise enhanced load carrying capacity due to the strengthening offered by the sheet overlap in the floor design. These hollow panel systems meet the Australian standard specifications for construction load limits showing direct application as a ready to use working platform or for temporary floor components in modular construction. The following points summarise the structural performance of the newly proposed lightweight flooring panels:

(i) The overlap of sheets improves the stiffness of the panels in bending, thereby increasing the load-carrying capacity.
(ii) Triple cell panels achieved 55% higher loads than double cell panels of the same overall dimensions.
(iii) Panels with mid-plate achieved 76% more load than panels without mid-plate due to simultaneous double skin action.
(iv) The flexural failure, local buckling and failure of slots are prominent types of failure observed in various types of specimen configurations used in this study.

The observed deficiencies in the hollow panels can be rectified by infilling these modular components with sustainable cementitious materials such as ultra-high performance concrete [25], geopolymer concrete [26], etc., for structural flooring applications.

Author Contributions: Conceptualisation, K.H., R.A.-A.; Methodology, K.J., S.R., B.K., M.W., K.H., M.E., N.U., M.R.H., R.A.-A.; Formal Analysis, K.J., S.R.; Investigation, K.J., S.R.; Resources, K.H.; Writing—Original Draft Preparation, K.J., S.R.; Writing—Review & Editing, B.K., R.A.-A.; Supervision, B.K., M.W., K.H., M.E., N.U., M.R.H., R.A.-A.; Project Administration, R.A.-A., B.K.; Funding Acquisition, R.A.-A., M.R.H. All authors have read and agreed to the published version of the manuscript.

Funding: The authors acknowledge the research fund from Deakin University, Victoria, Australia. In addition, the authors acknowledge the in-kind support by industry partners L2U Pty. Ltd. and FormFlow, Australia.

Institutional Review Board Statement: Not applicable.

Informed Consent Statement: Not applicable.

Data Availability Statement: The data presented in this study are available on request from the authors.

Acknowledgments: The authors acknowledge the technical support by the industry partners L2U Pty. Ltd., and FormFlow, Australia. The authors also gratefully acknowledge the Technical Staff—Lube Veljanoski and Michael Shanahan for their support and assistance to complete the experimental investigation at the Structures Laboratory, Deakin University.

Conflicts of Interest: The authors declare no conflict of interest.

References

1. Fiume, F.; Callegaro, N.; Albatici, R. Modular Construction for Emergency Situation: A Design Methodology for the Building Envelope. In *Sustainability and Automation in Smart Constructions*; Springer: Cham, Switzerland, 2021; pp. 131–141. [CrossRef]
2. Gatheeshgar, P.; Poologanathan, K.; Gunalan, S.; Shyha, I.; Sherlock, P.; Rajanayagam, H.; Nagaratnam, B. Development of affordable steel-framed modular buildings for emergency situations (Covid-19). In *Structures*; Elsevier: Amsterdam, The Netherlands, 2021; Volume 31, pp. 862–875. [CrossRef]
3. Zhang, Y.; Lei, Z.; Han, S.; Bouferguene, A.; Al-Hussein, M. Process-oriented framework to improve modular and offsite construction manufacturing performance. *J. Constr. Eng. Manag.* **2020**, *146*, 04020116. [CrossRef]
4. Lin, T.; Lyu, S.; Yang, R.J.; Tivendale, L. Offsite construction in the Australian low-rise residential buildings application levels and procurement options. *Eng. Constr. Archit. Manag.* **2021**. [CrossRef]
5. Dai Pang, S.; Liew, J.R.L.; Dai, Z.; Wang, Y. Prefabricated Prefinished Volumetric Construction Joining Tech-niques Review. *Modul. Offsite Constr. (MOC) Summit Proc.* **2016**. [CrossRef]
6. Hussein, M.; Eltoukhy, A.E.; Karam, A.; Shaban, I.A.; Zayed, T. Modelling in Off-Site Construction Supply Chain Management: A Review and Future Directions for Sustainable Modular Integrated Construction. *J. Clean. Prod.* **2021**, *310*, 127503. [CrossRef]
7. Choi, J.O.; Chen, X.B.; Kim, T.W. Opportunities and challenges of modular methods in dense urban environment. *Int. J. Constr. Manag.* **2019**, *19*, 93–105. [CrossRef]
8. Liew, J.; Chua, Y.; Dai, Z. Steel concrete composite systems for modular construction of high-rise buildings. In *Structures*; Elsevier: Amsterdam, The Netherlands, 2019; Volume 21, pp. 135–149. [CrossRef]
9. Jang, J.; Ahn, S.; Cha, S.H.; Cho, K.; Koo, C.; Kim, T.W. Toward productivity in future construction: Mapping knowledge and finding insights for achieving successful offsite construction projects. *J. Comput. Des. Eng.* **2021**, *8*, 1–14. [CrossRef]
10. Ferdous, W.; Bai, Y.; Ngo, T.D.; Manalo, A.; Mendis, P. New advancements, challenges and opportunities of multi-storey modular buildings–A state-of-the-art review. *Eng. Struct.* **2019**, *183*, 883–893. [CrossRef]
11. Wang, L.; Webster, M.D.; Hajjar, J.F. Behavior of deconstructable steel-concrete shear connection in composite beams. *Struct. Congr. 2015* **2015**, 876–887. [CrossRef]
12. Gunawardena, T. Behaviour of Prefabricated Modular Buildings Subjected to Lateral Loads. Ph.D. Thesis, University of Melbourne, Melbourne, Australia, 2016.
13. Boadi-Danquah, E.; Robertson, B.; Fadden, M.; Sutley, E.J.; Colistra, J. Lightweight modular steel floor system for rapidly constructible and reconfigurable buildings. *Int. J. Comput. Methods Exp. Meas.* **2017**, *5*, 562–573. [CrossRef]
14. Hosseini, M.R.; Chileshe, N.; Rameezdeen, R.; Lehmann, S. Integration of design for reverse logistics and harvesting of information: A research agenda. *Int. J. Logist. Syst. Manag.* **2015**, *20*, 480–515. [CrossRef]
15. Vaz-Serra, P.; Wasim, M.; Egglestone, S. Design for manufacture and assembly: A case study for a prefabricated bathroom wet wall panel. *J. Build. Eng.* **2021**, *44*, 102849. [CrossRef]
16. Razkenari, M.; Fenner, A.; Shojaei, A.; Hakim, H.; Kibert, C. Perceptions of offsite construction in the United States: An investigation of current practices. *J. Build. Eng.* **2020**, *29*, 101138. [CrossRef]
17. Brunesi, E.; Nascimbene, R. Numerical web-shear strength assessment of precast prestressed hollow core slab units. *Eng. Struct.* **2015**, *102*, 13–30. [CrossRef]
18. Hosseini, M.R.; Martek, I.; Zavadskas, E.K.; Aibinu, A.A.; Arashpour, M.; Chileshe, N. Critical evaluation of off-site construction research: A Scientometric analysis. *Autom. Constr.* **2018**, *87*, 235–247. [CrossRef]
19. John, K.; Ashraf, M.; Weiss, M.; Al-Ameri, R. Experimental investigation of novel corrugated steel deck under construction load for composite slim-flooring. *Buildings* **2020**, *10*, 208. [CrossRef]
20. Arrayago, I.; Real, E.; Mirambell, E.; Marimon, F.; Ferrer, M. Experimental study on ferritic stainless steel trapezoidal decks for composite slabs in construction stage. *Thin-Walled Struct.* **2019**, *134*, 255–267. [CrossRef]
21. FormFlow. 2020. Available online: https://formflow.net.au (accessed on 13 December 2021).
22. Madsen, T.; Hansen, K.H. Building System. U.S. Patent 8,539,730 B2, 2013.

23. Lysaght Customflow. 2021. Available online: https://www.lysaght.com/products/customflow (accessed on 13 December 2021).
24. Lysaght. 2021. Available online: https://cdn.dcs.lysaght.com/download/lysaght-build-on-inspiration-design-in-steel (accessed on 13 December 2021).
25. Liao, J.; Yang, K.Y.; Zeng, J.-J.; Quach, W.-M.; Ye, Y.-Y.; Zhang, L. Compressive behavior of FRP-confined ultra-high performance concrete (UHPC) in circular columns. *Eng. Struct.* **2021**, *249*, 113246. [CrossRef]
26. Rahman, S.K.; Al-Ameri, R. A newly developed self-compacting geopolymer concrete under ambient condition. *Constr. Build. Mater.* **2021**, *267*, 121822. [CrossRef]